STUDY OF THE INTERFACE MATRIX-INCLUSION PROPERTIES ON FRACTURE PROPERTIES IN COMPOSITE MATERIALS

Eduardo Bittencourt
Universidade Federal do Rio Grande do Sul
Departamento de Engenharia Civil
Av. Osvaldo Aranha, 99, Porto Alegre, RS – 90035-190
Brazil
Bittenco@cpgec.ufrgs.br

Adrián Cisilino
Universidad Nacional de Mar del Plata - CONICET
División Soldadura y Fractomecánica – INTEMA
Av. Juan B. Justo 4302 – (7600) Mar del Plata
Argentina
cisilino@fi.mdp.edu.ar

Abstract. *The addition of a second phase (inclusions) in a homogeneous matrix can modify significantly the global behavior of the composite depending on geometry (dimensions and distribution) and physical properties of the second phase. The analysis of the composite behavior can be done through the determination of the so called "representative volume" that permits to define a new constitutive homogeneous tensor that characterizes the behavior of the whole composite. However, due to obvious limitation in terms of mesh, this procedure may lose information about the interaction between matrix and second phase (debonding for instance). Also, if the second phase is plastic, it will probably cavitate. The study presented in this work consists in the analysis of a single unit cell consisting in a cylindrical domain containing a spherical inclusion. The matrix of the material is PMMA, which is considered as linear elastic. The second phase (the inclusion) is rubber and is considered elasto-plastic. Experimental studies performed on PMMA specimens have demonstrated that the addition of rubber particles results in a substantial increment in toughness. This increase in the material toughness apparently comes from the existence of holes inside the PMMA matrix (regardless the presence of rubber) and in the cavitation of the rubber due to plastic strains. The plastic strain dissipates energy and promotes crack arrest. However, the cavitation may be inhibited by the occurrence of debonding between matrix and the rubber inclusion. The influence of all these variables on toughness will be studied using a finite element code that considers debonding. The algorithm used is based on the so called cohesive interface method (Needleman (1987)). Preliminary results show that debonding may reduce significantly toughness by eliminating plastic strain of the cavitation.*

Keywords*: debonding, cavitation, PMMA, rubber, finite element*

1. Introduction

PMMA (polymethyl-methacrylate) is a brittle glassy polymer that has a great applicability in many fields of engineering mainly because its transparency. To overcome the problems related to brittleness, it is common the addition of rubber as a second phase. These blends are usually called rubber-toughned PMMA or simply RT-PMMA. Usually it is necessary the addition of at least 15 % of rubber to have a noticeable effect on toughness. The addition of rubber is done through spherical particles. To keep as much as possible the transparency of the blend, sometimes the particles also contains shells of PMMA (core-shell particles).

Experimental or qualitative information is available related to this composite (Fasce et al (2004)). It is known that the addition of rubber is important for toughening by two mechanisms: the arrest of propagating cracks and the energy dissipation due to plastic deformation. At the crack tip, where a hydrostatic state of stress exists, plastic strains are possible due to the cavitation of the rubber particles (Steenbrink, Van der Giessen (1997)). Cavitation or plastic deformations in the rubber particles are not possible if debonding occurs in the interface between matrix and rubber.

Quantitative or numerical analysis of the phenomena described above applied to RT-PMMA blends are difficult to find. To the author's knowledge, only a few references to the works by Todo and co-workers (Todo et al. (2000), Todo et al. (2001)) are available. On the other hand, researches concerning other polymer blends are abundant. These works investigate aspects related to the rubber properties (yield stress, hardening, etc), the size effect of the particles and the effect of the hydrostatic stresses.

In what follows the effects of the stress triaxiality, the rubber mechanical properties and the particle size on the overall toughness of the material are investigated by means of FEA. The algorithm used is based on the so called cohesive interface method (Needleman (1987)) and allows for debonding in the matrix-particle interface. Crazing is not considered. Regarding notation, "{ }" and "[ ]" are used to identify vectors and matrices respectively; "." is used for scalar products.

2. Constitutive Law

The interface between two different materials is able to support tractions $\{T\}$ through the introduction of cohesive elements between the faces of both materials. The methodology follows the works developed by Needleman and co-workers (see for instance Needleman (1987) and Xu and Needleman (1994)). Considering an interface opening $\{\Delta u\}$ in bi-dimensional problems, $\{n\}$ the normal vector and $\{t\}$ the tangent vector to the interface, it can be defined that:

$$\Delta_n = \{\Delta u\}\cdot\{n\} \qquad T_n = \{T\}\cdot\{n\} \tag{1}$$

and

$$\Delta_t = \{\Delta u\}\cdot\{t\} \qquad T_t = \{T\}\cdot\{t\} \tag{2}$$

A cohesive normal traction arises as a result of the opening according to the phenomenological relations below (for a null tangent opening):

$$T_n = -\frac{\phi_n \Delta_n}{\delta_n^2}\exp\left(-\frac{\Delta_n}{\delta_n}\right) \tag{3}$$

Equation (3) has a peak value ($\sigma_{\max}$) for a normal opening δ_n. The symbol ϕ_n is the well-known energy fracture per unit area of the crack for mode I opening. Integrating Eq. (3) in Δ_n, we have the energy dissipated during crack opening (or the area under the curve $T_n\, x\, \Delta_n$). For $\Delta_n >> \delta_n$, this integral is equal to the energy fracture ϕ_n and the cohesive traction T_n is zero, which means rupture of the interface. Replacing $\Delta_n = \delta_n$ in Eq. (3) we have:

$$\delta_n = \frac{\phi_n}{\exp(1)\sigma_{\max}} \tag{4}$$

The three variables in Eq. (4) are the fracture parameters for the interface. Then only two of these variables are independent. $\sigma_{\max}$ corresponds to the peak stress on the crack tip and, for ductile (elasto-plastic) materials, its value is around $3\, x\, \sigma_y$ where σ_y is the yield stress.

A cohesive tangent traction is also considered. In this case, considering a null normal opening, we have:

$$T_t = -2\frac{\phi_n \Delta_t}{\delta_n^2}\exp\left(-\frac{\Delta_t^2}{\delta_n^2}\right) \tag{5}$$

In this equation it was considered that ϕ_t (the energy fracture per unit area of the crack for mode II) is equal to ϕ_n.

The PMMA is considered an elastic Hookean material, while the rubber is elasto-plastic. The rate of deformation [D] for the rubber can be written as (assuming small elastic rate of deformation):

$$[D] = [D^e] + [D^{pl}] \tag{6}$$

Where [D^e] is the elastic part and [D^{pl}] is the plastic part of the rate of deformation. To calculate [D^{pl}] a flow-rule/von Mises type constitutive law is used:

$$[D^{pl}] = \Lambda[N] \tag{7}$$

where,

$$[N] = \frac{[\sigma']}{\sqrt{[\sigma']\cdot[\sigma']}} \tag{8}$$

and

$$\Lambda = \frac{[N]\cdot[D]}{\left(1+\frac{h}{3G}\right)} \tag{9}$$

$[\sigma']$ is the deviatoric stress, h is the hardening modulus and G is the shear modulus. σ_y is updated using the evolution equation below:

$$\sigma_y = \sigma_y^0 + h\bar{\varepsilon}^{pl}$$

where σ_y^0 is the initial yield stress and $\bar{\varepsilon}^{pl}$ is the equivalent plastic strain. For both materials, objective stress rate $\left[\overset{\nabla}{\sigma}\right]$ is calculated as:

$$\left[\overset{\nabla}{\sigma}\right] = [\Psi][D^e] \tag{10}$$

where $[\Psi]$, for the rubber, is the constitutive law that comes out from Eq. (6) to (9). For PMMA, $[\Psi]$ is the Hooke law. Equation (10) together with Eq. (3) and (5) form the constitutive laws for the volume and interface respectively. These constitutive laws were introduced in a finite element code in order to study the blend behavior.

3. Discretization

The model adopted here for the RT-PMMA is only an approximation of the real case. Assuming hexagonal packets of PMMA with rubber spheres, as depicted in the Fig. 1(a), a two-dimensional (axisymmetric) model of one packet can be considered (Fig. 1(b)). Due to symmetry only one fourth of the axisymmetric model was considered as marked in gray in the Fig. 1(b).

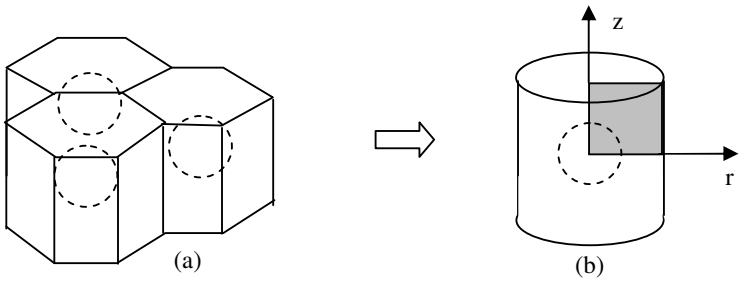

Figure 1. Axisymmetric approximation (b) of the real situation (a)

The Finite Element mesh used is depicted in Fig. (2). Iso-parametric four nodes bi-linear elements were used. Cohesive elements are considered only between rubber and PMMA.

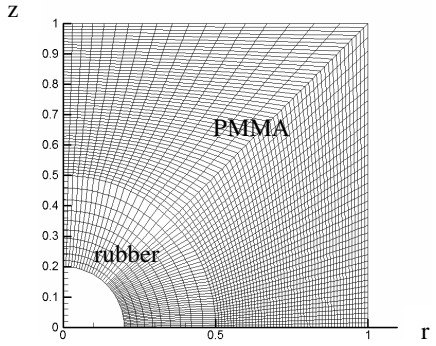

Figure 2. Finite element mesh used in all cases

Observe that an initial void is considered inside the rubber particle. So nucleation of the void is not an issue considered in this work. The growth of the void by plastic strain however may occur depending on stress condition and this is the main toughening effect caused by the rubber. Observe that if debonding occurs it will play an important hole in the void growth and therefore in toughness. These aspects, as well as physical and geometrical properties of the materials will be explored below. The volumetric fraction of the rubber (plus void) is 16,5 % in all analyses performed here. No periodic boundary conditions were considered.

Loading is prescribed throughout prescribed displacements on radial (r) and axial (z) direction in order to have different level of triaxiality along the interface.

Equilibrium equations were solved using the explicit Central Difference method (see Hughes (1987))

4. Examples

The basic parameter that was analyzed in following the examples are the plastic strains in the rubber or the dissipated energy. No considerations regarding stiffness of the blend were made. Boundary conditions, rubber properties, size of the rubber particles will be changed in order to investigate how they modify dissipation of energy. Properties of the PMMA will not be changed. Energy dissipation will be considered only qualitatively by considering the density of plastic energy ξ, which will be calculated as follows:

$$\xi = \sum_{1}^{n} \sigma_y \bar{\varepsilon}^{vp}$$

where n is the number of nodes in the mesh. PMMA properties are always E=3240 MPa (elastic modulus), ν=0.35 (poisson coefficient). For the rubber, E=1450 MPa, ν=0.49, σ_y^0 = 20 MPa, h=500 MPa. The interface properties were considered as taken from rubber, then $\sigma_{\max} = 3 x \sigma_y^0 =$ 60 MPa.

4.1. Effect of applied triaxiality

Figure 3 shows iso-values of plastic strains for (a) radial prescribed displacements only and (b) a ratio of axial to radial prescribed displacement equal to 0.73 (such a relation in terms of stress is representative of the stress state ahead of the crack tip). We can observe that in the case (a) there is not debonding and an elevated degree of plasticity occurs in the rubber (until 46%). For case (b) debonding occurs in early stages of the loading process, reducing significantly the level of plasticity. The pattern of plastic strain is also different in both cases. In case (a) plasticity occurs mostly in internal poles of the rubber, while in case (b) a radially uniform distribution of plastic strain developed before propagation of the crack at the interface, as can be see in Fig. 4(a). With crack propagation, plasticity will still advance. However, as can be seen in Fig. 4(b), as only the poles remain bonded to the matrix, there is a tendency of localization of plastic strain at approximately 45 degrees. The deformation of the rubber can be an important clue to understand how it crazes, phenomenon we did not explore here.

Figure 5 shows that the dissipated energy, ξ, is different for both cases. It can be concluded that the stress triaxiality reduce significantly the toughness of the blend by inducing debonding. It can be seen that a total debonding of the rubber particle occurred before 2% of total radial deformation. It is interesting to note that experimental evidences (see Riziera et. al) report extensive debonding at such level of deformation.

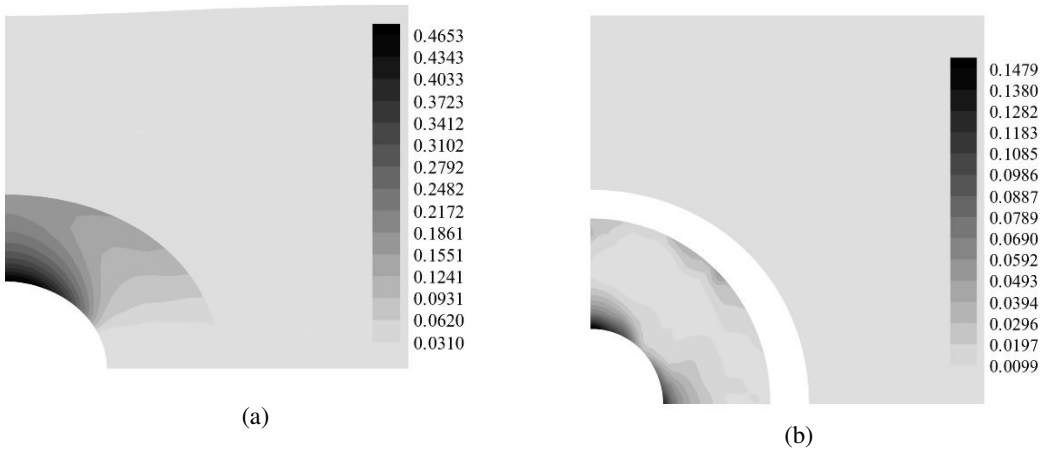

Fig. 3: Effect of triaxiality. Iso-values of equivalent plastic strains $\bar{\varepsilon}^{pl}$ shown: (a) only radial displacements applied; (b) radial and axial displacements applied (final configuration)

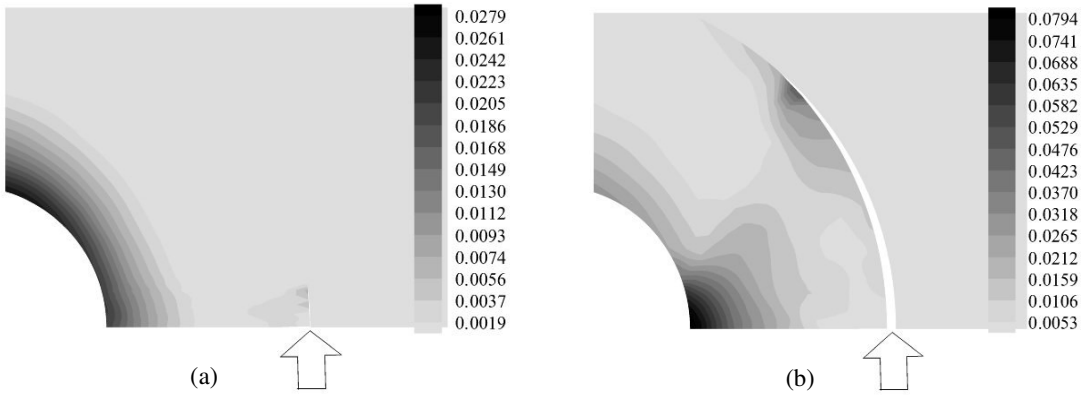

Fig. 4: Evolution of equivalent plastic strains and debonding when triaxiality is present. (a) beginning of debonding; (b) intermediate configuration (arrow indicates interface position).

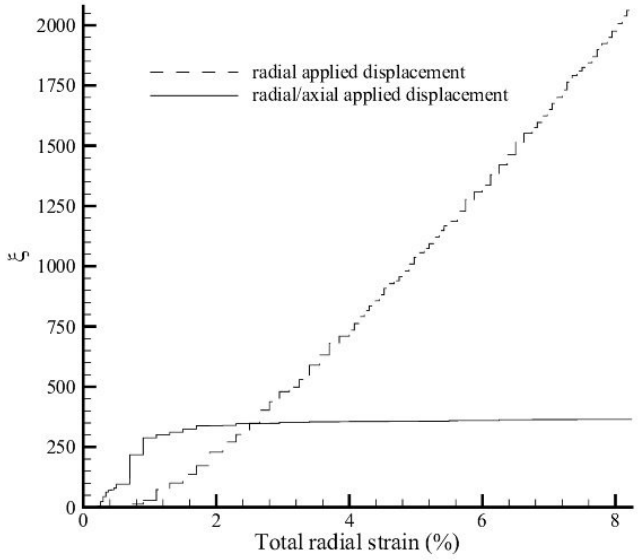

Fig. 5: Effect of triaxiality on the density of dissipated energy ξ

4.2. Effect of rubber properties

Figure 6 shows the changes in the density of dissipated energy ξ for different combinations of rubber properties. (In all cases in this item, the axial/radial displacement ratio is 0.73.) For the set of curves with similar final value of ξ, rubber properties were changed (yield stress and hardening) and interface properties were kept constant. Then it can be concluded that no significant change in toughness is trigged by the rubber properties alone. However, when the interface properties are linked to rubber properties, we can see a considerable increase in toughness (curve at the top in Fig. 6) when yield stress of the rubber is increased. It is clear then that this effect is due to increase of $\sigma_{\max}$ of the interface. (Observe that in all cases, ϕ_n is not changed)

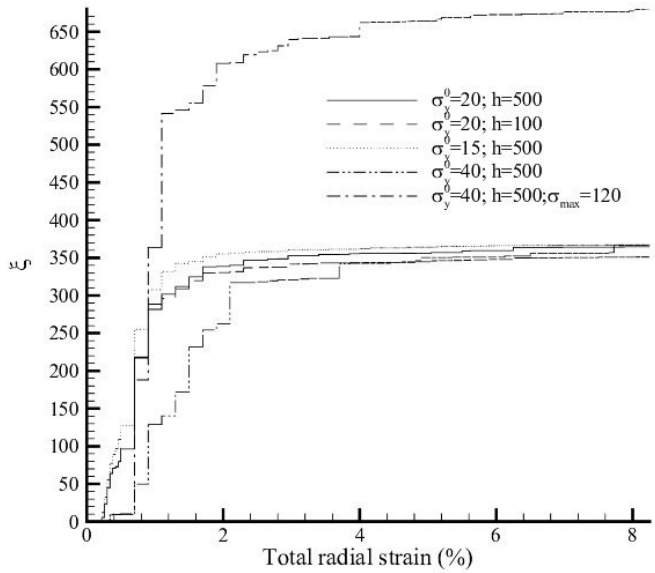

Figure 6. Effect of rubber properties on the density of dissipated energy ξ. When not indicated $\sigma_{\max}$ = 60 (All values in MPa)

4.3. Size effects

Observe that the fracture methodology used in this work introduce a characteristic length (δ_n) in the formulation that may capture the effect of the particle size on toughness. Two situations were analysed with this purpose: R/δ_n=2500 and R/δ_n=250 (R is the particle radius). All other properties were considered the same. (To change the ratios, mesh - or R - was uniformly reduced ten times in order to keep always the same interface properties). The results are shown in Fig. 7 and it can be observed that smaller inclusions lead to a greater toughness. This is a well-known qualitative property of composites that would not be captured numerically if the formulation did not include a characteristic length.

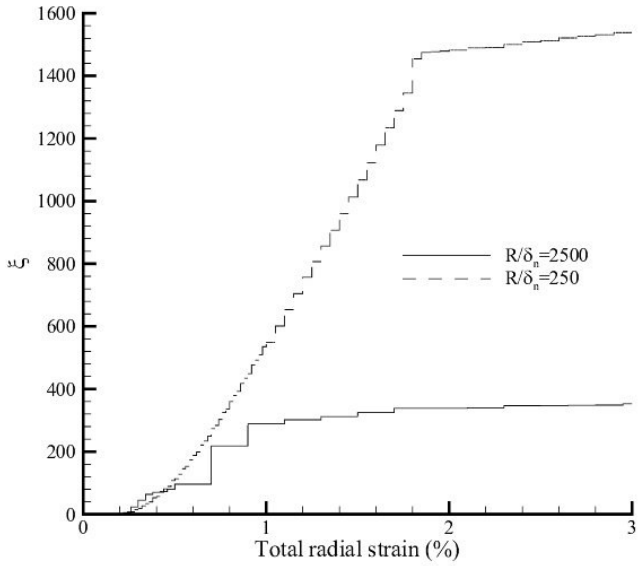

Figure 7. Effect of the radius (R) of the particles on the density of dissipated energy ξ.

5. Concluding Remarks

The effect of loading, rubber properties and particle size were numerically analysed in this work for a RT-PMMA blend. Obtained results allowed to conclude:

- Stress triaxiality has a strong effect on debonding of the rubber particles, reducing drastically cavitation or plasticity of them. The blend is then much less though.
- Rubber properties seem to have a minor effect on toughness, but a more detailed study of this matter should be done. If interface properties are directly linked to rubber properties, an increased toughness can be obtained increasing the yield stress of the rubber.
- The smaller the rubber particles, the tougher is the blend. (This aspect could be captured because the numerical methodology used introduces a characteristic length). The conclusion confirms the general trend in continuum mechanics, regarding microstructure sizes, that "smaller is better".

6. Acknowledgements

CAPES (Brazil) and Grant PICT 12-12528 of ANPYCT (Argentina) partially funded this research.

7. References

Fasce L.A., Pettarin V., Seltzer R. and Frontini P.M., 2003, “Evaluation of impact fracture toughness of polymeric materials by means of the J-integral approach”, Polymer Engineering & Science, Vol. 43/5, pp. 1081-1095.

Ghassemieh, E., 2002, “Micro-mechanical analysis of bonding failure in a particle-filled composite”, Composite Science and Technology, Vol. 62, pp 67-82.

Hughes, T.J.R., 1987, “The Finite Element Method”, Prentice-Hall, Englewood Cliffs, 803 p.
Needleman, A., 1987, “A continuum model for void nucleation by inclusion debonding”, J. of Appl. Mech., Vol. 54, pp. 525-531.
Rizzieri, R., Crawshaw, J., Donald, A.M., Bucknall, C.B. and Moore D.R., 2005, “Studies of deformation mechanisms in rubber toughened PMMA to elucidate the role of the rubber particles in the toughening process”, http://www.mmc.espci.fr/resumespubli/Seminaire_rizzieria.htm
Steenbrink, A.C. and Van der Giessen, E., 1997,” A Numerical Study of Cavitation and Yield in Amorphous Polymer-Rubber Blends”, Journal of Eng. Mat. And Tech., Vol. 119, pp 256-261.
Todo, M. and Takahashi, K., 2001, “Loading-Rate Dependence of Mode I Fracture Behavior of Rubber-Toughened PMMA”, Proceedings of the 10th International Conference on Fracture, CD-ROM.
Todo, M., Arakawa, K. and Takahashi, K., 2000, “Nonlinear Displacement Field in the Vicinity of Notch-Tip in Rubber Toughened PMMA”, Key Engineering Materials, Vol.183-187, pp.409-414, 2000.
Xu, X.P. and Needleman, A., 1994 “Numerical Simulations of Fast Crack Growth in Brittle Solids”, J. Mech. Phys. Solids, Vol. 42, pp. 1397-1424.

8. Responsibility notice

The authors are the only responsible for the printed material included in this paper.